LA-UR- 97-4273

CONF-9710155--

Los Alamos National Laboratory is operated by the University of California for the United States Department of Energy under contract W-7405-ENG-36

TITLE: MOLECULAR DYNAMICS SIMULATIONS OF GRAIN BOUNDARIES IN THIN NANOCRYSTALLINE SILICON FILMS

AUTHOR(S): G.P. Berman, T-13
D.K. Campbell, Univ of Illinois
G.D. Doolen, T-13
V.A. Luchnikov, Russian Academy of Sci
R. Mainieri, T-13

SUBMITTED TO: ULTRA ELECTRONICS AND ADVANCED MICROELECTRONICS PROGRAM REVIEW, 26-31 OCTOBER, 1997, SANTA FE, NM

Los Alamos

Los Alamos National Laboratory
Los Alamos, New Mexico 87545

FORM NO. 836 R4
ST. NO. 2629 5/81

October 16, 1997

Molecular Dynamics Simulations of Grain Boundaries in Thin Nanocrystalline Silicon Films

G.P. Berman[1], D.K. Campbell[2], G.D. Doolen[1], V.A. Luchnikov[1,3], R. Mainieri[1]

[1] *Theoretical Division, T-13, and Center for Nonlinear Studies, Los Alamos National Laboratory, Los Alamos, New Mexico 8545, U.S.A.*

[2] *Department of Physics, University of Illinois at Urbana-Champaign, 1110 West Green St., Urbana, IL 61801-3080, U.S.A.*

[3] *Institute of Chemical Kinetics and Combustion, Russian Academy of Sciences, 630090 Novosibirsk, Russia*

Using molecular dynamics simulations, the grain boundaries in thin polycrystalline silicon films (considered as promising material for future nanoelectronic devices) are investigated. It is shown that in polysilicon film with randomly oriented grains the majority of grain boundaries are disordered. However, some grains with small mutual orientation differences can form extended crystalline patterns. The structure of the grain boundaries satisfies the thermodynamical criterion suggested in [23]. The majority of atoms in the grain boundaries are tetrahedrally coordinated with the nearest neighbors, even though the grain boundaries are disordered. The grain boundary matter is characterized as an amorphous phase with a characteristic tetragonality value.

I. Introduction

Recently it was demonstrated that thin polycrystalline silicon films can be considered as promising material for room temperature single-electron devices [1]- [4]. There are at least two reasons which make this material attractive:

I). Usually, the film's thickness varies from 1 to 5 nm, and the average lateral grain size is 10 nm or less. In this case, the energy of an electron in a single grain, E_e, is larger than the thermal energy even at room temperature, $E_e > T = 300^o K$.

II). It is believed that in these films, the characteristic resistance of the potential barriers between the grains is sufficiently large, $R_b > R_c = h/e^2 \sim 25k\Omega$. If both these conditions are satisfied, an electron can be strongly localized in the grain. At the same time, one can regulate (up to some extent) the electron conductivity in these films by varying the gate voltage, and creating a current channel. Those electrons which are stored in the grains (quantum dots) create a Coulomb repulsion for those electrons which are involved in the current channel. This allows one to implement memory operations in these films at room temperature using a Coulomb blocade effect. Different implementations of these ideas are discussed, for example, in [1]- [4]. The boundaries between the nanocrystalline grains in these films play important role in satisfying the two conditions mentioned above. For example, one of the most important characteristics of the electron transport in polysilicon films is connected with the distribution of crystalline and amorphous grain boundaries (GB) [5].

At room temperature, the main factor which determines the structure of a GB is the mutual orientation difference between neighboring crystalline grains. It is conventionally accepted to consider a GB as a low-angle one if one interatomic extraction between the grains accumulates on more than approximately five interatomic distances in the GB plane [6]. In this case, the GB can be represented as a sequence of crystalline defects. Such a GB remains crystalline up to 90% of the melting temperature of the bulk crystal [7]. Increasing the misorientation angle increases the difficulty of forming crystalline structure between the neighboring grains. The large-angle GBs are normally disordered.

The distribution of structures in grain boundaries, in principle, should correlate with the distribution of orientations of individual crystalline grains, which can be affected by many factors, such as the thickness of the polysilicon film [8], application of the electromagnetic field during crystallization [9,10], etc.

However, there is no standard geometrical criteria which would allow one to predict the structure of a GB from the value of the misorientation angle. The structures of the GBs depend not only on this angle, but also on the type of the misorientation. The misorientation has many degrees of freedom: the boundary can be asymmetric, it can be tilted or twisted, or both. For some of the high-angle misorientations, the neighboring grains can fit each other at the GB plane. In this case, the GB can be highly ordered [11]. Because of these reasons there does not exist a consistent theoretical approach to the description of GBs.

In this situation, a large-scale molecular dynamics (MD) simulation of thin polysilicon film can provide valuable information. The initial polycrystalline film can be constructed using an assumption about the distribution of the orientations of the polycrystalline grains. Then, after relaxation at given temperature, the structure of the GBs can be directly observed.

In this paper, we present preliminary results of MD simulations of GBs in thin polysilicone film, at room temperature. In sections II and III, we describe the MD procedure and the results of simulations of a single GB between two crystals with "medium – angle" misorientations. In Section IV, we discuss the results of modelling thin (3.1 nm) polysilicon film, constructed using the assumption of random orientations of the grains, with several grains having small misorientations. In Section V, we summarize the results.

II. The Bicrystal Model and the Simulation Procedure

In this section, we study the tilt symmetrical bicrystal boundary close to (1 1 1) crystallographic plane. This is one of the most important boundaries for silicon [12]. In particular, the symmetrical twin (1 1 1)-boundaries are known to have very low energy, and they are

the most frequently observed GBs in the polysilicon films [13]. To prepare the initial configuration of the bicrystal system, we first generated its top half, so that the (X, Y)-plane in the model's system of coordinates is close to the (1 1 1)-interface (Fig. 1). Namely, the bottom of our model corresponds to the (8 8 5)-crystallographic plane which has an angle of 11.4^o with the (1 1 1)-plane. The length and the width of the model box were chosen so that periodic boundary conditions occur in X – and Y – directions. In the Z – direction, we used free boundary conditions, allowing the system to change its volume during relaxation. The lower half of the bicrystal was constructed by mirror reflection of the top half, so the total misorientation angle is, $\alpha = 22.8^o$. Then from every pair of close atoms (which coincide or closer than $0.9a$ to each other; here $a = 0.235\ nm$ is the nearest distance between atoms in bulk crystal silicon, at $T = 0$) one atom was removed to avoid very high potential energies. The final configuration contained 6768 atoms, and had the dimensions $2.30 \times 9.49 \times 6.29\ nm$. One interatomic distance misfit between the two halves of the bicrystal accumulates every $\sim$ 2.5 interatomic distances along Y-direction in the boundary plane. According to the criterion described in the Introduction, this GB can be considered to be a "medium-angle" one. Because of the relatively small value of α, the condition of periodicity requires much larger size of the system in Y – direction than in X – direction.

Relaxation of the system was performed by the standard MD simulation, in three stages. During the first 3000 time steps, the system was relaxed at $T = 10^o\ K$ in order to allow the boundary atoms to shift into positions with lower potential energy. During this procedure the interaction between atoms was a modified Stillinger-Weber (SW) potential [14], in which $(cos\ \theta + \frac{1}{3})^2$ was replaced by $(cos\ \theta + \frac{1}{3})^2 + \eta(cos\ \theta + \frac{1}{3})^4$. This modification, suggested by Dodson [15], doesn't change considerably the equilibrium properties of the crystal and amorphous models of the silicon (for which the SW potential is in good agreement with the experiment [14,16]). However, it emphasizes the role of the tetragonal coordination of atoms during formation of new covalent bonds. The value of parameter η is somewhat arbitrary; in our MD simulation we used $\eta = 0.3$ which in [17] was found to be reasonable for preventing dangling bonds in MD modelling of amorphous silicon. Then, the temperature

was elevated to $T = 300^o\ K$, and the system was relaxed during 5000 MD steps using the original SW potential. Finally, the system was quenched to zero temperature in order to eliminate thermal noise.

The equations of motion were integrated by the Verlet algorithm [18] with time-step $\delta t = 7.6634 \cdot 10^{-16} sec$ (0.01 in the reduced units). To keep a desired temperature, we used the Berendsen scaling temperature procedure [19]. For the initial relaxation of the GBs and for the final quenching to absolute zero, we used a short temperature relaxation time $\tau_q = 0.1\ ps$. At $T = 300^o\ K$, we used the temperature relaxation time $\tau_T = 1\ ps$. In order to keep a zero pressure in all directions, the X – and Y – dimensions of the system were allowed to vary during the simulation, according to the Berendsen scaling mechanism [19]. For the pressure relaxation time we used the value $\tau_P = 1\ ps$. We estimated the values of τ_T and τ_P from our preliminary study of relaxation times in a model of bulk crystal silicon. The isotermal compressibility of the system, in the inteval of temperatures studied, was estimated as $\beta = 0.6$.

II. Structure of the Bicrystal Grain Boundary

Fig. 2 shows the (Y, Z)-projection of our bicrystal model prepared using the MD simulation procedure described above. The bonds between the atoms are shown according to a distance criterion: a pair of atoms is connected by a bond if they are separated less than 0.26 nm. One can see that the GB was formed as a crystalline one with the localized defects periodically repeating along the Y – direction. The defects appear when the misfit between the halves of the bicrystal becomes untolerable for covalent bonds of the crystalline 6 – fold rings. In this case, atoms in positions with large misfit reorganize themselves into configurations with relatively low potential energy, by forming 5 – and 7 – fold rings.

Formation of these rings requires only small distortions of the tetragonal coordination of atoms [20], so the atoms participating in them have only slightly higher average potential energy than in the bulk crystal phase. This is demonstrated in Fig. 2a by coloring the atoms according to potential energy, and in Fig. 3 by the profile of potential energy per

atom along the Z – direction, averaged by 0.2 nm thick layers parallel to the GB plane. Blue in Fig. 2a indicates those atoms whose potential energy u_j (the bond energy, $u_j = u_j^{(2)} + u_j^{(3)}$, where $u_j^{(2)}$ and $u_j^{(3)}$ are the potential energies of the j-th atom in two – and three – atom interactions, correspondingly) is lower than or equal to $u^1 = -8.5\ eV$. This limit is slightly above the energy of atoms in a perfect crystal: $u^{(cr)} = -8.67\ eV$. Green indicates those atoms for which $u^1 < u_j \leq u^{(a)}$, where $u^{(a)} = -7.9\ eV$ is the average potential energy of atoms in the bulk amorphous phase at $T = 0^o\ K$; the value $u^{(a)}$ (as well as other values for the MD models of amorphous and liquid silicon) was obtained from the models explored in [17]. With red we indicate the atoms for which $u_j > u^{(a)}$.

Atoms with the highest energy (up to $-5.5\ eV$) are located on the free surfaces of the bicrystal. A relatively small fraction of the boundary atoms also have high energies, up to approximately $-7\ eV$. These atoms are located in those regions with the largest misfit between the halves of the bicrystal. One can see that the potential energy, u_j, of the majority of the boundary atoms belongs to the intermediate region between the energies of atoms in the bulk crystal and the bulk amorphous phase. Some atoms in the crystalline regions in the GB do not exceed the energies of atoms in the bulk crystal. As shown in Fig. 3, the average potential energy per atom, calculated in 0.2 nm-thick layers parallel to the GB plane, $U = \frac{1}{n_{layer}}\left(\frac{1}{2}\sum_{j\in layer} u_j^{(2)} + \frac{1}{3}\sum_{j\in layer} u_j^{(3)}\right)$, in the GB lies well below the cohesive energy of the bulk amorphous phase which is $U^{(a)} \simeq -4.15\ eV$ per atom.

Potential energy, u_j, of the atoms closely correlates with the degree of their tetragonal coordination with the nearest neighbors. To estimate the tetragonal coordination of the j-th atom we calculated the value,

$$\mathcal{T}_j = \sum_{l<k} \frac{(l_{jl} - l_{jk})^2}{15\overline{l_j}^2},$$

which is called the *tetragonality* [21]. Here l_{jk} is the length of k-th edge of the tetrahedron of general shape formed by the four nearest neighbors of the j-th atom; $\overline{l_j}$ is the average length of the edge. By definition, $\mathcal{T}_j$ is equal to zero for the ideal tetrahedron (diamond structure), and it increases if the shape of the tetrahedron is distorted. The value, $\mathcal{T}_j$, is correlated with

the dispersion of the edge lengths of the tetrahedron. According to the criterion suggested in [21], the spatial figure formed by four points can be recognized as having the "good tetrahedral shape" if $\mathcal{T}_j$ is less than or equal to $\mathcal{T}^{(c)} = 0.018$. The value of tetragonality of an atom is very sensitive to the number of atoms in the first coordination shell, z. In the bulk amorphous phase of silicon, for which $z_a \simeq 4.04$, the average tetragonality is equal to $\mathcal{T}_{am} = 0.015$ which is slightly less than the critical value $\mathcal{T}^{(c)}$. In liquid silicon (in which the first coordination shell consisits in average of $z_{lq} \simeq 4.46$ neighbors), the average value of tetragonality is, $< \mathcal{T} >_{lq} \simeq = 0.034$.

For the bicrystal model shown in Fig. 2, the profile of average (over the atomic layers parallel to the GB plane) tetragonality of atomic environment along the Z-direction is presented in Fig. 4. The largest values of $\mathcal{T}$ belong to the atoms located in the free surfaces for which the four nearest neighbors do not form a tetrahedron. Low values of $\mathcal{T}$ in the bulk crystal imply that at room temperature the thermal fluctuations almost do not change the tetragonal coordination of atoms in the regular crystal lattice. The neighborhood of GB atoms is normally tetrahedral, i.e., $\mathcal{T} < \mathcal{T}^{(c)}$. However, some atoms in the GBs have a value of $\mathcal{T}$ which is larger than the critical tetragonality, $\mathcal{T}^{(c)}$. As noted in [17] such atoms usually have dangling bonds or more than four nearest neighbors in the first coordination shell. As a consequence, the same atoms have the largest potential energy.

The density of atoms in the 0.6 nm–thick region belonging to the GB is slightly lower than the density of the perfect bulk perfect crystal: $\rho_{GB} = 2.239\ g/cm^3$ compared with $\rho_{crystal} = 2.327\ g/cm^3$. The GB region in our bicrystal model is also characterized by a noticable inhomogeneity of the spatial distribution of free volume, which we describe by the radii of interstitial spheres, R_i, [22]. The 7-fold rings surround comparatively large voids for which $R_{i(7)} \simeq 0.24\ nm$; that is approximately 9% larger than the radius of voids in the bulk crustal: $R_{i(cr)} \simeq 0.22\ nm$. At the same time, the 5-member rings surround relatively small voids, with $R_{i(5)} \simeq 0.21\ nm$; that is $\simeq 5\%$ smaller than the $R_{i(cr)}$. These deviations of the radii of interstitial spheres in the GB region are about 3 times larger than the thermal deviations of R_i in the bulk crystal at the room temperature. Thus, the spatial

inhomogeneity of the free volume in the GB is an essentual structural feature.

III. Model of Polysilicon Film

The initial configuration of the polysilicon film was generated using the Voronoi algorithm: first, the centers of the grains were defined; then each grain was obtained by filling the space, nearest to the center of the grain, with a diamond lattice with a chosen orientation. The atoms with very high potential energies were removed from the GBs in the same way as was done for the bicrystal GB. The film had the dimensions $16.7 \times 16.7 \times 3.1\ nm$, and contained 44174 atoms in 12 grains (Fig. 5). The majority of the grains in our model were oriented randomly, so they had both tilt and twist misorientations. The four grains, namely 3,4,7 and 8 were generated so that the misorientation tilt angle between the 3-rd and 4-th grains was $\alpha_{3-4} = 11.0^o$; between the 4-th and 7-th grains $\alpha_{4-7} = 11.0^o$; and between the 7-th and 8-th grains, $\alpha_{7-8} = 15.0^o$. The GB_{3-4} and the GB_{7-8} are close to (1,1,1)-interface, and the GB_{4-7} is close to (0,0,1)-interface. The (1,1,1)-planes in these four grains are perpendicular to the plane of the figure. The average linear dimension in the $X-Y$ plane of a grain in our model, $d_{gr} \simeq 4.8\ nm$, is of the same order as for the grains in a real polycrystalline silicon film obtained recently by thermal annealing of amorphous Si deposited from decomposing silane on a SiO_2 substrate [4]. As in the bicrystal model, periodic boundary conditions were used in X - and Y - directions, and free boundary conditions were used in Z - direction. The same MD procedure as described above, was applied for relaxation of the model.

In Table I, we present the data on the potential energy per atom, density and average tetragonality for the longest GBs (for which it was possible to make measurements with the reasonable accuracy). In Fig. 5 we show the final configuration of the polycrystalline film, with atoms coloured in accordance with their potential energy (Fig. 5a) and tetragonality (Fig. 5b). One can see that the GBs demonstrate large range of values. The GB between the 3–4 grains is crystalline, with a defect in the middle. Correspondently, this boundary has the lowest potential energy (see Table I). The boundary between the 7-th and the 8-th grains also contains distinguishable crystalline connections formed by the low-energy atoms.

For the same value of the misorientation angle, $\alpha = 11.0^o$, the atoms in the GB between the 4-th and the 7-th grains have, on average, larger potential energy than in the GB between the 3-rd and the 4-th grains. It appears that the energy of the GB tilt close to the (0 0 1)-interface is more sensitive to the misorientation angle than the energy of the GB tilt close to the (1 1 1)-interface.

Mostly disordered GBs, which are $\simeq 1\ nm$ thick, can be distinguished by the large fraction of the red atoms, whose potential energy exceeds the average potential energy of the atoms in the amorphous state, $u^{(a)}$. These GBs appear between grains with random mutual misorientation. However, in these GBs there are also many atoms with $u_j < u^{(a)}$. and, on average, the potential energies per atom of the GBs, $U^{(GB)}$, are close to the energy of the amorphous state, $U^{(a)}$.

Before the relaxation at $T = 300^o\ K$ (i.e. after the initial minimization of the potential energy) the potential energy per atom in the high-angle GBs exceeded the energy in a-Si by $\delta \sim 0.1\ eV$. Thus, the stability of the disordered GBs at $U^{(GB)} \simeq U^{(a)}$ means that the difference, δ, was a driving force of the amorphization of the GBs during the process of relaxation. At the same time, the process of relaxation only slightly changed the structure of the low-energy crystalline GBs. In this respect, the structure of the GBs in our polysilicon model satisfies the thermodynamical criterion, suggested recently by Keblinski, Phillpot and Wolf in [23]. According to this criterion, a GB remains crystalline if the potential energy of the boundary region does not exceed the potential energy of the bulk amorphous state; and becomes disordered otherwise.

Densities of the tilt crystalline GBs between grains 3, 4, 7 and 8 are practically the same, or slightly smaller, than the density of the bulk crystal, ρ_{cr}. The densities of other GBs are systematically larger than ρ_{cr}. In covalent materials with friable structure, such as silicon and germanium, some GBs, indeed, can contract. This was observed in X-ray diffraction experiments on (1 0 0) twist GBs in Ge [24] and in MD simulations of (1 1 1)-twist boundaries in silicon [25]. It is remarkable that the contraction is observed for the twist boundaries. In such GBs the covalent bonds are most probably stretched rather than squeezed, and the

system demonstrates a tendency to restore their lengths at the cost of a reduction of the GB's volume. In a system with the randomly oriented grains the GBs, obviously, both tilt and twist. The fact that in our system we observed the contraction of the majority of the GBs means that the influence of the twist misorientations is more essentual for the value of density in the GBs.

Dispite the fact that the density of the disordered GBs is slightly higher than the density of the amorphous silicon, Keblinski *et. al.* characterized the structure of the GB in their MD model of polysilicon as the amorphous phase [26]. This conclusion followed from a similarity between the behavior of local radial distribution functions, $g(r)$, in the GBs and $g(r)$ in the bulk amorphous silicon, as well as from the similarity of the corresponding bond-angle distributions. In our model, we also consider the disordered GBs as amorphous. From the data represented in Table I, and from the coloring of atoms in Fig. 5b one can see that the majority of atoms in the high-angle GBs are tetrahedrally coordinated. At the same time, these atoms are arranged in non-crystalline manner. The value of the average tetragonality in the GBs is about the same as the average tetragonality in amorphous silicon, $< \mathcal{T} >_a$, but much lower than the average tetragonality in the liquid silicon, $< \mathcal{T} >_{lq}$.

IV. Conclusion

MD simulation reveals useful information about the distribution of the structures of grain boundaries in polycrystalline silicon film. In our model of polysilicon film, the majority of the boundaries between grains with random mutual orientation are disordered. The grains with small mutual misorientations are connected by the crystalline grain boundaries. The grain boundaries with "medium-angle" misorientation, studied within a bicrystal model, have the complex inhomogeneous structure. These boundaries consist of crystalline connections separated by disordered regions. In disordered regions the misfit between the crystal structures of the neighboring grains is compensated by non-crystalline arrangements of atoms, such as 5- and 7-fold rings. In general, the structure of the grain boundaries satisfy the thermodynamical criterion suggested in [23].

The region of a tilt "medium-angle" grain boundary is characterized by considerable inhomogeneity in the spatial distribution of the free volume. The variations of the radii of the interstitial spheres reaches in our model up to 9% of the mean value.

The potential energy of silicon atoms is closely correlated with tetragonality, $\mathcal{T}$, of their coordination with the nearest neighbors. The majority of atoms in polysilicon grain boundary are tetrahedrally coordinated, even if they are arranged in non-crystalline manner in the high-angle grain boundary. From the fact of relatively small values of average tetragonality of atoms, it follows that the high-angle disordered grain boundaries can be characterized as amorphous.

The results obtained are important for understanding the structural properties of thin polycrystalline silicon films, which have been used recently for memory nano-devices. However, for obtaining more reliable data, larger polysilicon simulations should be considered.

Acknowledgements

We would like to thank D.K. Ferry and P. Lomdahl for useful discussions. This work was supported by the Linkage Grant 93-1602 from the NATO Special Programme Panel on Nanotechnology, and by the Defense Advanced Research Projects Agency.

REFERENCES

[1] K. Yano, T. Ishii, T. Hashimoto, T. Kobayashi, F. Murai, K. Seki, *Extended Abstracts of the 1994 Int. Conf. on Sol. State Devices and Matter.*, 325-327 (1994).

[2] K. Yano, T. Ishii, T. Hashimoto, T. Kobayashi, F. Murai, K. Seki, *IEEE Transactions on Electron Devices.* **41**, 1628 (1994).

[3] S. Tiwari, F. Rana, H. Hanafi, A. Hartstein, E.F. Crabbé, K. Chan, *Appl. Phys. Lett.*, **68**, 1377 (1996).

[4] A.H.M. Kamal, J. Lützen, B.A. Sanborn, M.V. Sidorov, M.N. Kozicki, D.J. Smith, D.K. Ferry, *subm. to SST*, 1997.

[5] S. Nomura, X.W. Zhao, Y. Aoyagi, T. Sugano, *Phys. Rev. B*, **54**, 13974-13979 (1996)

[6] J.P. Hirth, J. Lothe, *Theory of Dislocations, New York*, 1982.

[7] I.Nguyen,Y.Sidney, *Mat. Sci. and Engineering*, **A107**, 15-22 (1989)

[8] C.V.Thompson, *Mat. Res. Soc. Symp. Proc.*, **343** 3-12 (1994).

[9] K.S.S.Reddy, M.Satyam, *Sol. State Comm.*, **93** 797-799 (1995).

[10] Y.J.Park, E.K.Kim, M.H.Son, S.-K.Min, *J. of Cryst. Growth*, **156** 487-490 (1995).

[11] G.Hasson, J.-Y.Boos, I.Herbeuval, M.Biskondi and C.Goux, *Surf. Sci.*, **31**, 115-137 (1972).

[12] V.G. Lifshits, A.A. Saranin, A.V. Zotov, *Surface phases of silicon*, John Wiley & Sons, England, 1994.

[13] D. Shechtman, J.L. Hutchison, L.H. Robins, E.N. Farabaugh, A. Feldman, *J. Mater. Res.*, **8**, 473 (1993).

[14] F.H. Stillinger, T.A. Weber, *Phys. Rev. B*, **31**, 5262 (1985).

[15] B.W. Dodson, *Phys. Rev. B*, **33**, 7361 (1986).

[16] M.D. Kluge, J.R. Ray, A. Rahman, *Phys. Rev. B*, **36**, 4234 (1987).

[17] V.A. Luchnikov, N.N. Medvedev, A. Appelhagen, A. Geiger, *Mol. Phys.*, **88**, 1337 (1996).

[18] W.C. Swope, H.C. Andersen, P.H. Berens, K.R. Wilson, *J. Chem. Phys.*, **76**, 637 (1982).

[19] H.J.C. Berendsen, J.P.M. Postma, W.F. van Gunsteren, A. DiNola, J.R. Haak, *J. Chem. Phys.*, **81**, 3684 (1984).

[20] D.E. Polk, *J. of Noncryst. Sol.*, **5**, 365 (1971).

[21] N.N. Medvedev, Yu.I. Naberukhin, *J. Noncrystalline Solids*, **94**, 402 (1987).

[22] An interstitial sphere is a sphere of maximal radius constrained by the centers of four atoms and which does not contain the centers of any other atoms of the system. For a more detailed explanation see, for example, N.N. Medvedev, V.P. Voloshin, Yu.I. Naberukhin, *J. Phys. A*, **21**, L24 (1988).

[23] P. Keblinski, S.R. Phillpot, D. Wolf, H.Gleiter *Phys. Rev. Lett.*, **77**, 2965 (1996).

[24] P.Lamarre, F.Schmückle, K.Sickafus and S.L.Sass, *Ultramicroscopy*, **14**, 11 (1984).

[25] S.R.Phillpot, D.Wolf,*Phil. Mag. A*, **60**, 545 (1989).

[26] P.Keblinski, S.R.Phillpot, D.Wolf and H.Gleiter, *Acta mater.*, **45**, 987-998 (1997)

	GB_{3-4}	GB_{4-7}	GB_{7-8}	GB_{3-6}	GB_{6-7}	GB_{4-1}	GB_{1-5}	GB_{5-2}	GB_{9-10}	GB_{10-11}	GB_{9-12}	$a-Si$	$cr-Si$
$U\ (eV/at), \pm 0.04$	−4.24	−4.18	−4.20	−4.19	−4.16	−4.17	−4.18	−4.09	−4.21	−4.15	−4.14	−4.15*	−4.335
$\rho\ (g/cm^3), \pm 0.02$	2.29	2.31	2.34	2.39	2.39	2.41	2.38	2.36	2.37	2.38	2.38	2.29*	2.324
$< \mathcal{T} >, \pm 0.0003$	0.005	0.014	0.011	0.010	0.013	0.013	0.011	0.017	0.012	0.015	0.017	0.015*	0

Table I: Potential energy, density and average tetragonality of grain boundaries in the polysilicon model. * Data for a-Si obtained from the model [17]

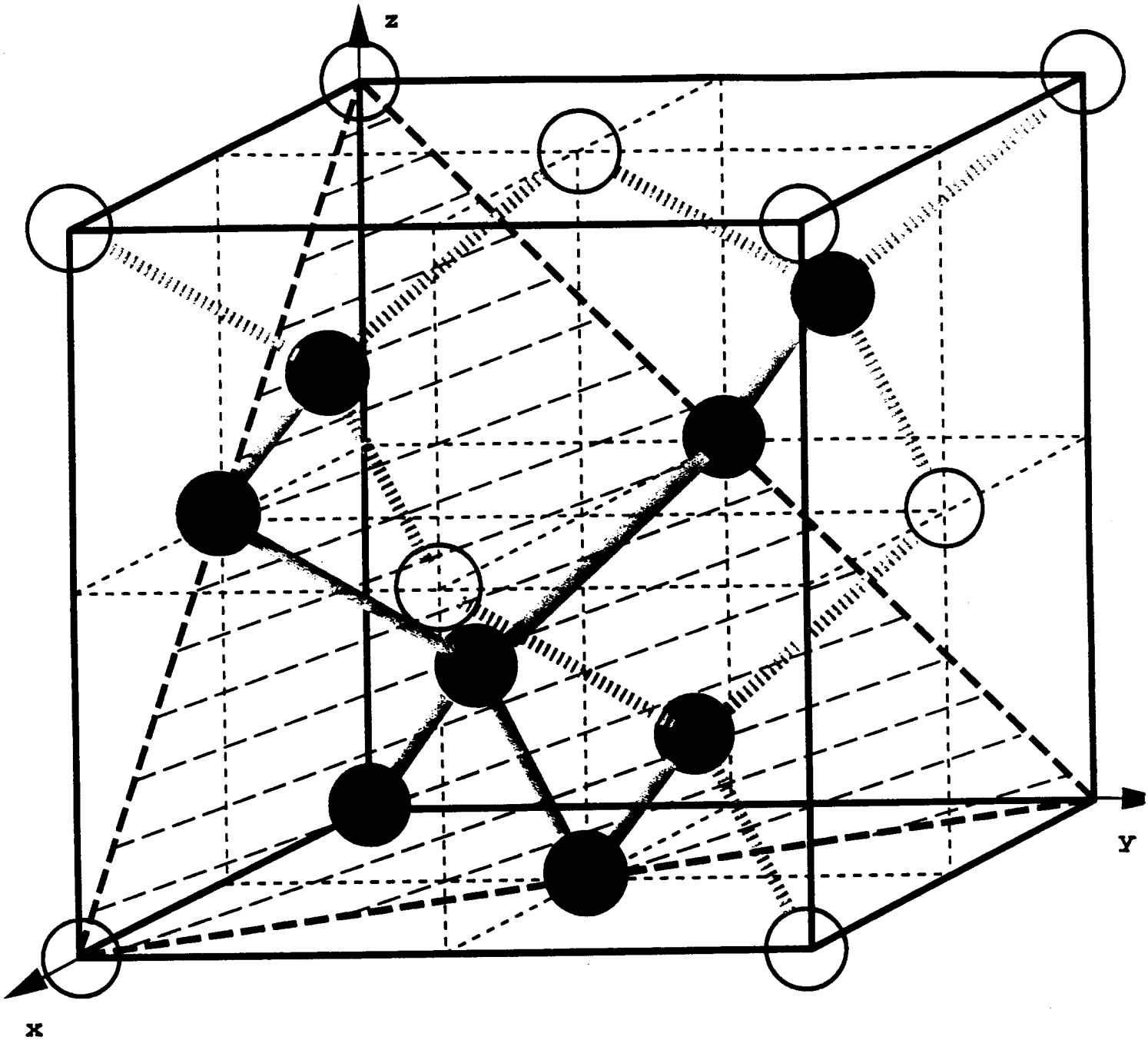

Fig. 1a. Generation of the bicrystal model: one elementary cell of the diamond structure, and position of (111)-crystallographic plane.

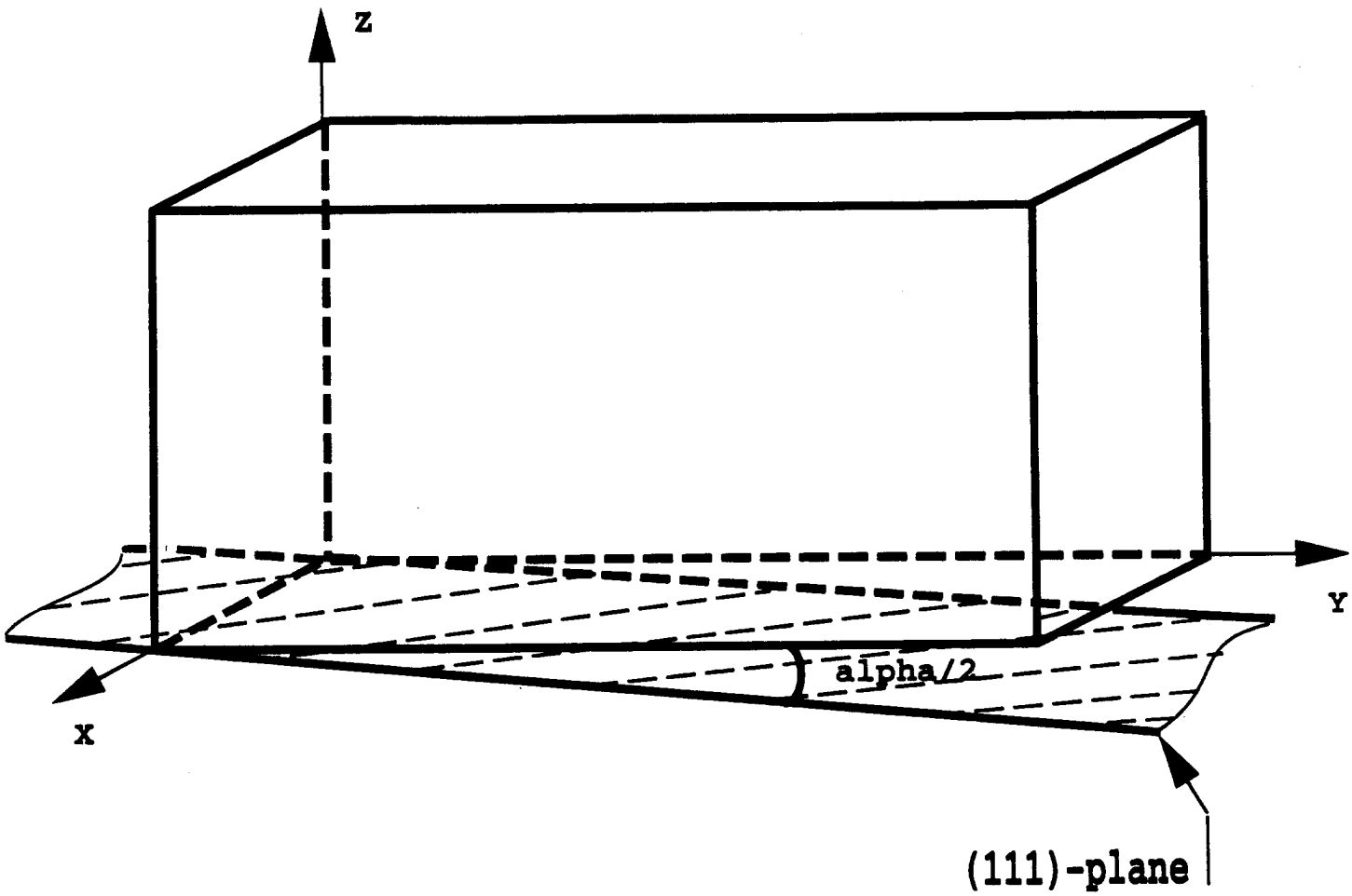

Fig. 1b. Generation of the bicrystal model: position of the top half of a bicrystal model relatively to the (111)-plane.

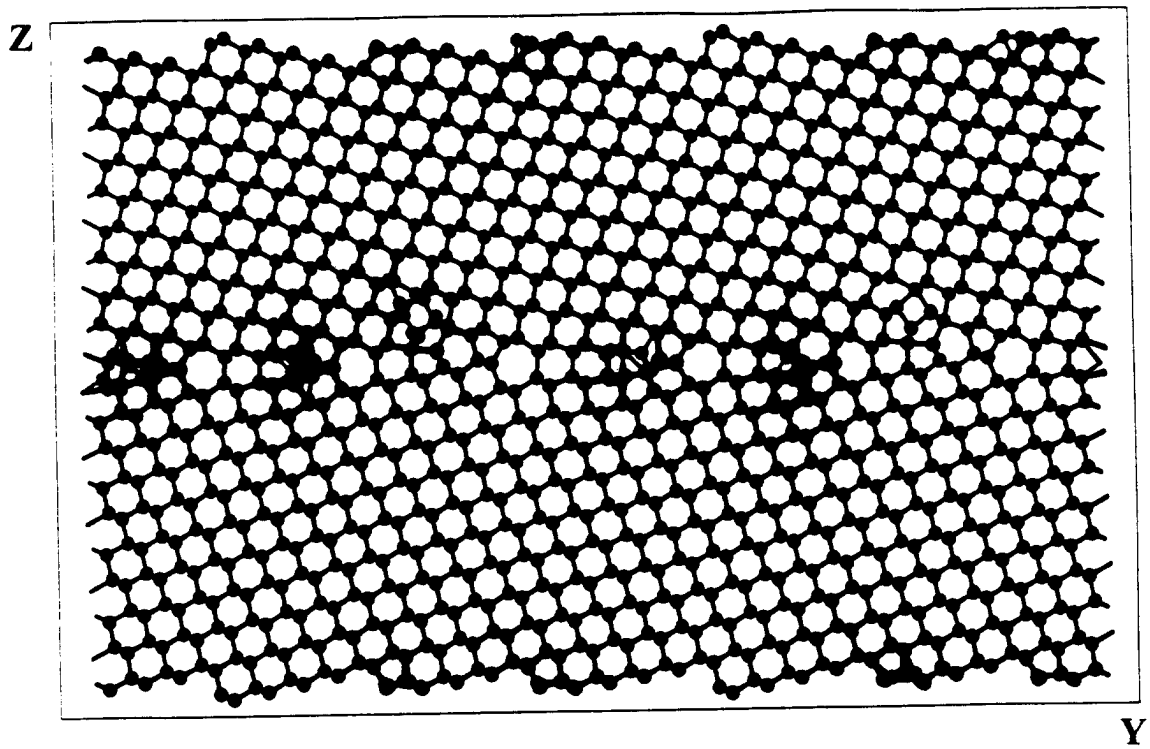

Fig. 2a. Projection of the bicrystal model onto the (Y,Z)-plane. The misorientation angle is $\alpha = 22.8^o$. The bonds are shown between the atoms which are less than 0.26 nm from each other. The color of the atoms indicates their potential energies:

blue: $u < -8.5\ eV$;

green: $-8.5eV < u < -7.9\ eV$;

red: $u > -7.9\ eV$

(for crystal Si : $u = -8.67\ eV$; for amorphous Si: $< u > = -7.9\ eV$).

The number of atoms: 6768. Temperature: $T = 300\ K$. Free boundary conditions are used in the Z-direction. Periodic boundary conditions are used in the X- and Y-directions. There are 11 atomic layers in the X-direction. The Stillinger-Weber potential is used.

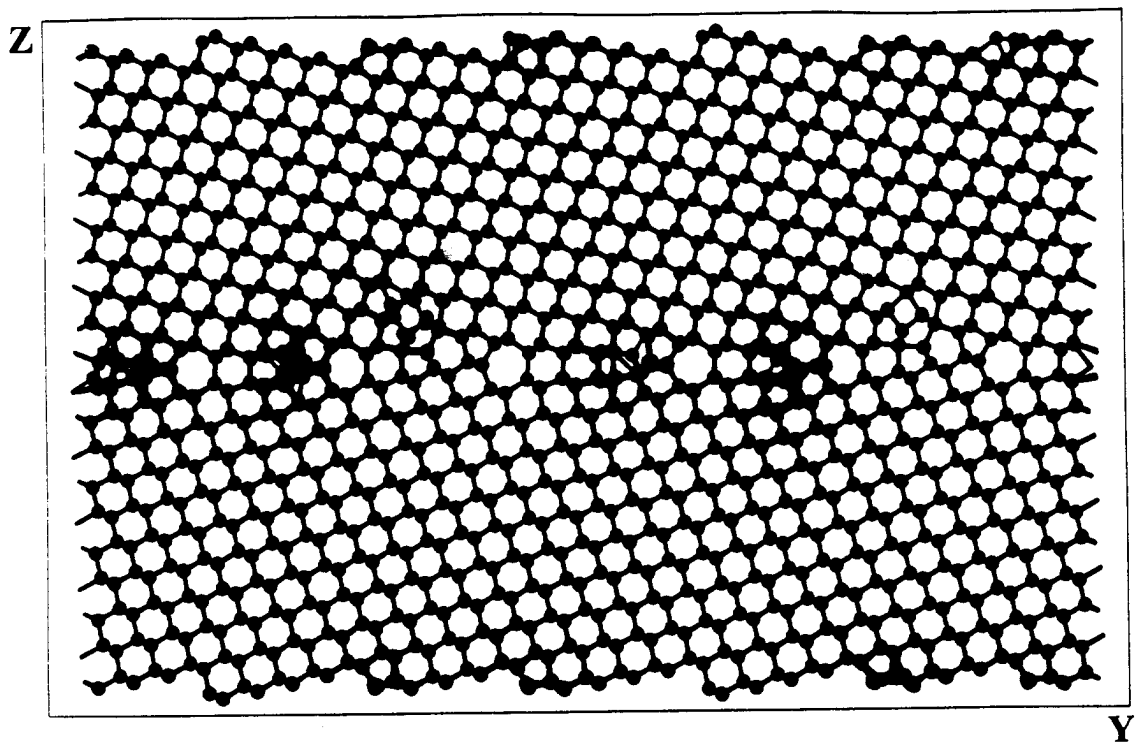

Fig. 2 b. Projection of the bicrystal model on the (Y,Z)-plane. Color of atoms indicates the degree of tetragonality, $\mathcal{T}$, of their coordination:

blue: $\mathcal{T} < 0.003$;

green : $0.003 < \mathcal{T} < 0.018$;

red : $\mathcal{T} > 0.018$

(for good tetrahedral coordination: $\mathcal{T} < 0.018$; for crystal Si: $\mathcal{T} = 0$; for amorphous Si: $< \mathcal{T} >= 0.015$).

Parameters are the same as in Fig. 2a.

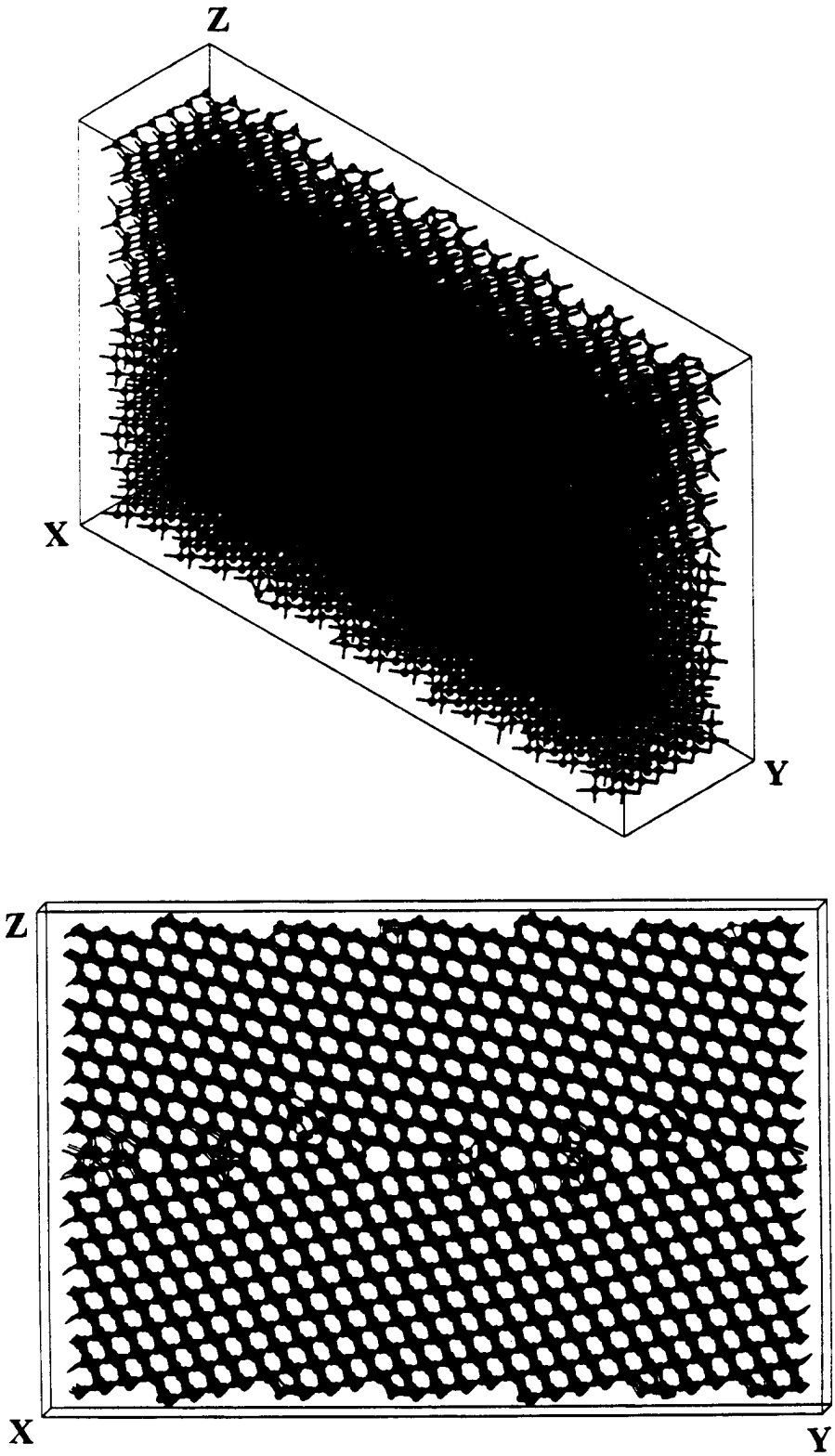

Fig. 2c. Bondary between two silicon crystals, two different projections. The atoms are colored according to their potential energy, u. Parameters are the same as in Fig. 2a and 2b.

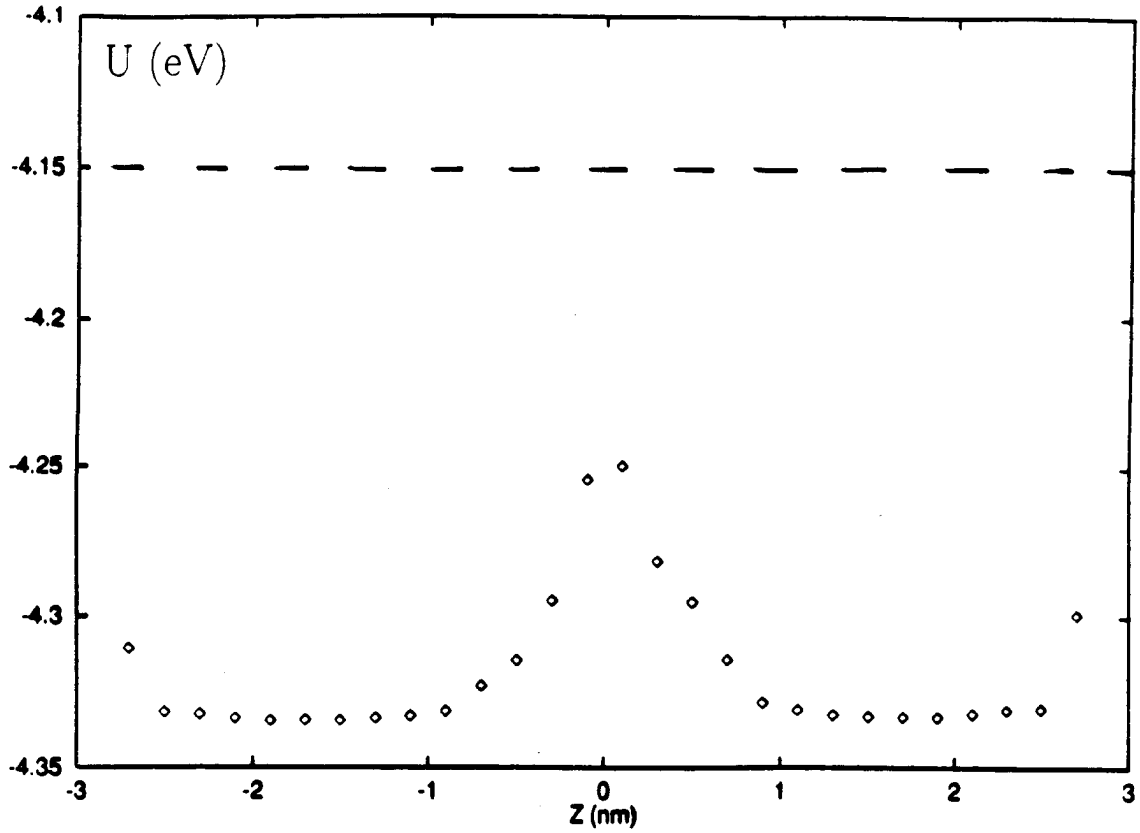

Fig. 3. Profile of potential energy per one atom, U, in Z – direction. Dashed line indicates the potential energy of the bulk amorphous phase, per one atom. Parameters are the same as in Fig. 2.

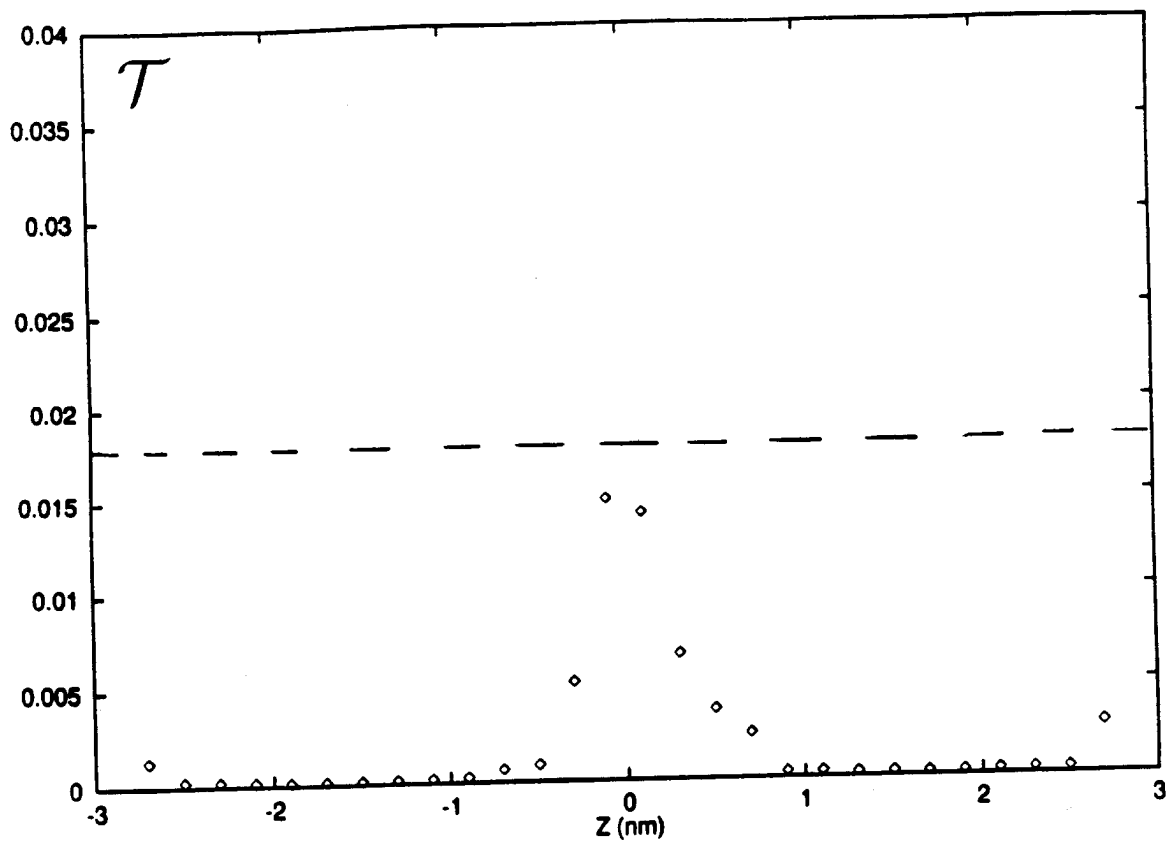

Fig. 4. Profile of tetragonality of the bicrystal model in Z – direction. Dashed line indicates the critical value of $\mathcal{T}$ for tetrahedra. Parameters the same as in Figs. 2 and 3.

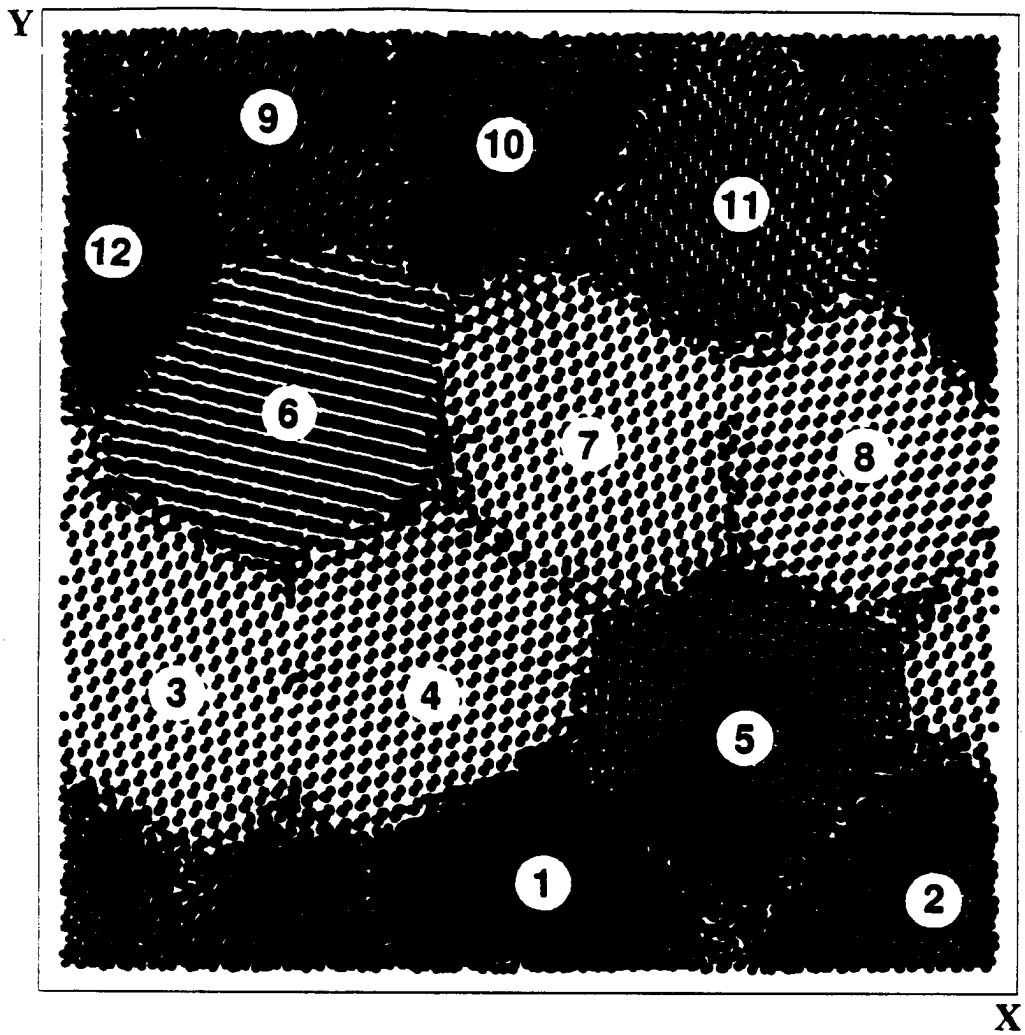

Fig. 5a. (X,Y)-projection of the polycrystalline film. Atoms are colored according to their potential energies, u, by the same rules as in Fig. 2a. Numbers numerate the crystalline grains.

The number of atoms: 44174. Size: $16.7 \times 16.7 \times 3.1$ nm. Temperature: $T = 300$ K. Free boundary conditions in the Z-direction; periodic boundary conditions in the X- and Y-directions. There are 15 atomic layers in Z-direction. Atoms on the free surfaces are not shown.

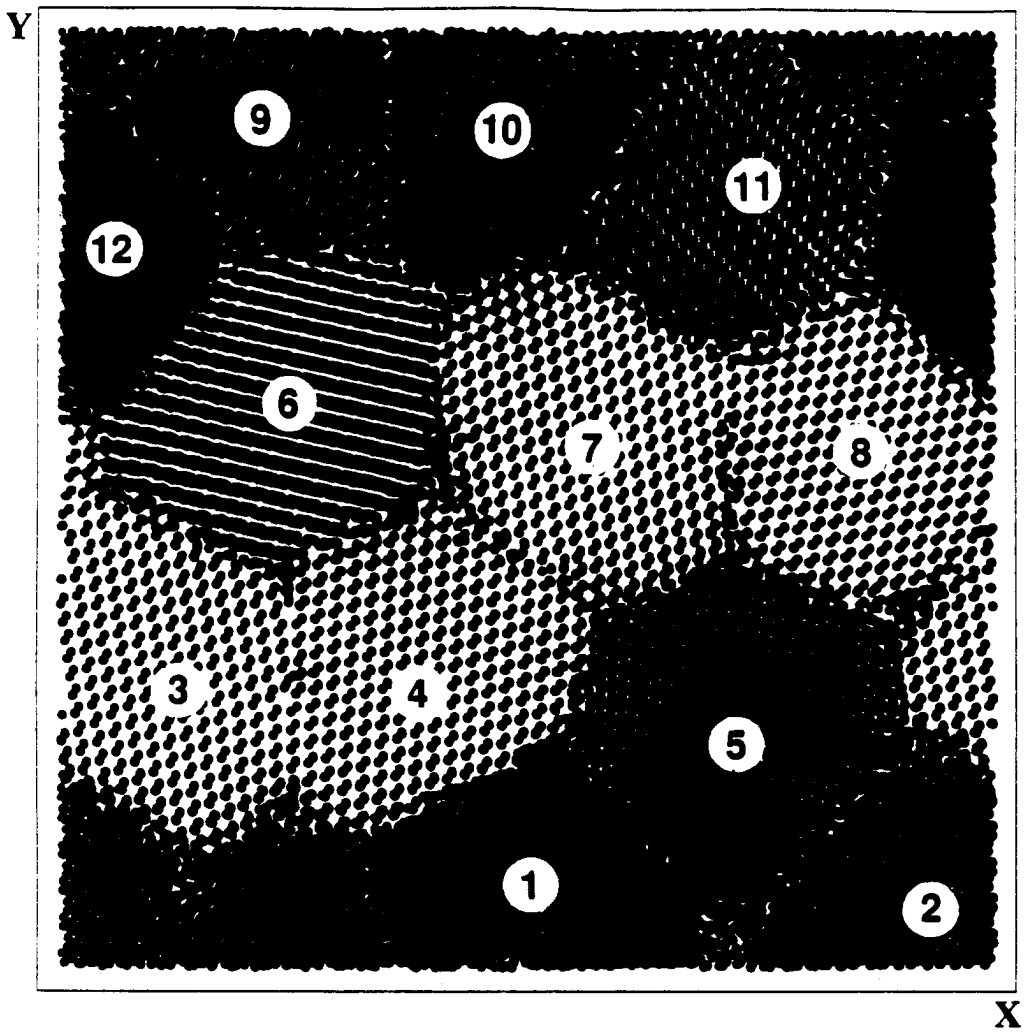

Fig. 5b. (X,Y)-projection of the polycrystalline film. Color indicate tetragonality, $\mathcal{T}$, as in the Fig. 2b. Parameters are the same as in Fig. 5a.

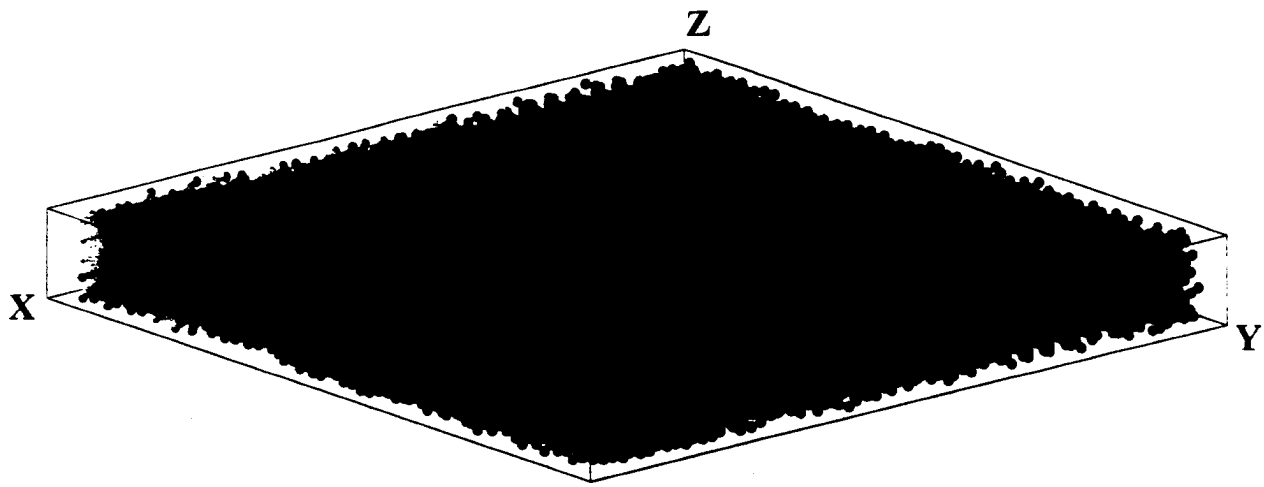

Fig. 5c. Three-dimensional view of the polycrystal model. Parameters are the same as in Fig. 5a and Fig. 5b.

Report Number (14) LA-UR--97-42 '73
CONF-970155--

Publ. Date (11) 199712
Sponsor Code (18) DOE/MA, XF
JC Category (19) UC-910, DOE/ER